A Gas Film Lubrication Study Part I Some Theoretical Analyses of Slider Bearings

Abstract: The Reynolds differential equation describing flow in a compressible lubricating film is developed. Important characteristics of such films are determined directly from the Reynolds Equation. Pressure, load, velocity, and geometry characteristics are presented for many compressible slider bearing films based upon computer solutions of a Reynolds difference equation as derived in Part II. Part III cites experimental verification of computer solutions and describes experimental techniques.

Introduction

Within the past decade, sharpened interest in gaseous lubrication has developed throughout the world. The gaslubricated bearing has been widely used to good advantage. For example, there have been applications in which low friction characteristics are required; applications in which there are large temperature variations, and it is desired that viscosity increase or remain nearly constant with temperature; applications in which the lubricant should not be adversely affected by radiation; applications in which an essentially fixed clearance between slider bearings and moving surface must be maintained under various conditions of acceleration; and applications in which ambient air can be used as a clean, available, inexpensive lubricant.

A hydrodynamic lubricating film is defined as that fluid which separates surfaces, with no internal sources or sinks, which have relative motion. By contrast, the term externally pressurized or hydrostatic film is sometimes used when internal sources are provided such that there will be no surface contact in the absence of relative surface motion.

The theory of hydrodynamic film lubrication, first proposed by Osborne Reynolds,¹ has been verified many times. Although occasional experimenters have found that they could not achieve a satisfactory correlation between theory and experiment, others have demonstrated that good correlation results by properly accounting for all significant boundary conditions and physical variables. For example, Part III of this series discusses experimental techniques used to verify theoretical characteristics of air-lubricated slider bearings.

The governing differential equations for compressible fluid flow for a laminar isotropic Newtonian fluid involve the velocity \mathbf{v} ; absolute pressure p; density ρ ; coefficient of viscosity μ ; dilatational (or bulk) viscosity λ ; film thickness or clearance h, between bearing and moving surface; absolute temperature T; specific heats c_p and c_v ; time t; and the body force \mathbf{F} . The equation of motion for the lubricating fluid is

$$\rho(\mathbf{v}_t + \mathbf{v} \cdot \nabla \mathbf{v}) = F - \nabla[\rho - (\frac{2}{3}\mu + \lambda)\nabla \cdot \mathbf{v}] + \mu\nabla^2\mathbf{v}, \qquad (1)$$

in which the subscript represents differentiation.

When the first order kinetic theory may be applied, the relation

$$\frac{2}{3}\mu + \lambda = 0 \tag{2}$$

is assumed. Then Eq. (1) takes the Stokes form, often called the Navier-Stokes equation. Since the region of interest is free from singularities, the continuity relation

$$\rho_t + \nabla \cdot (\rho \mathbf{v}) = 0 \tag{3}$$

may be used. In general, the energy equation

$$\rho g \mathbf{v} \cdot \nabla E + \rho \nabla \mathbf{v} = \nabla \cdot (K \nabla T) + \mu \Phi \tag{4}$$

is also necessary to provide a solution, in which the intrinsic energy per unit mass is given by

$$E=c_vT$$
,

and the dissipation function by

$$\Phi = 2(u_x^2 + v_y^2 + w_z^2) + (v_x + u_y)^2 + (w_y + v_z)^2 + (u_z + w_x)^2 - (\frac{2}{3})(\nabla \cdot \mathbf{v})^2.$$

Equations (1), (3), and (4) are sufficient, when combined with

$$p = \rho RT, \tag{5}$$

the equation of state for a perfect gas (or an appropriate pressure density relation for a liquid), and the necessary boundary conditions, to describe most laminar lubricating films.

The differential equations of a lubricating film

Figure 1 is a possible configuration for a film-lubricated slider bearing. The film thickness, h(x, y), ordinarily symmetrical with respect to the x, z plane, has a minimum clearance h_m . Widest interest centers on the case in which the surface, z=0, is assumed to move with velocity U in the x direction. The breadth of the bearing in the direction of surface motion is B, and the length normal to this motion is L. Since the surfaces usually deviate only slightly from being parallel, fluid velocity components normal to the surfaces may generally be disregarded. The configuration is similar to the film which might exist between two nearly parallel planes which are mathematically smooth, equal in size to football fields, and separated by one-half inch at one end, one inch at the other.

Fluid body forces are invariably negligible for the ordinary lubricating film. Additionally, for thin film thicknesses (h/B generally less than 10^{-3}), the inertia terms of Eq. (1) are usually negligible. This may be seen by writing a modified Reynolds number,

$$R^* = \frac{\rho u B}{\mu} \left(\frac{h}{B}\right)^2,$$

which has an order of magnitude equal to the ratio of inertia to viscous acceleration terms. When $R^* << 1$, and conditions are steady, the simplified classical lubrication

equations may be applied. With these restrictions, Eq. (1) reduces to

$$\nabla p = \mu \nabla^2 \mathbf{v} . \tag{6}$$

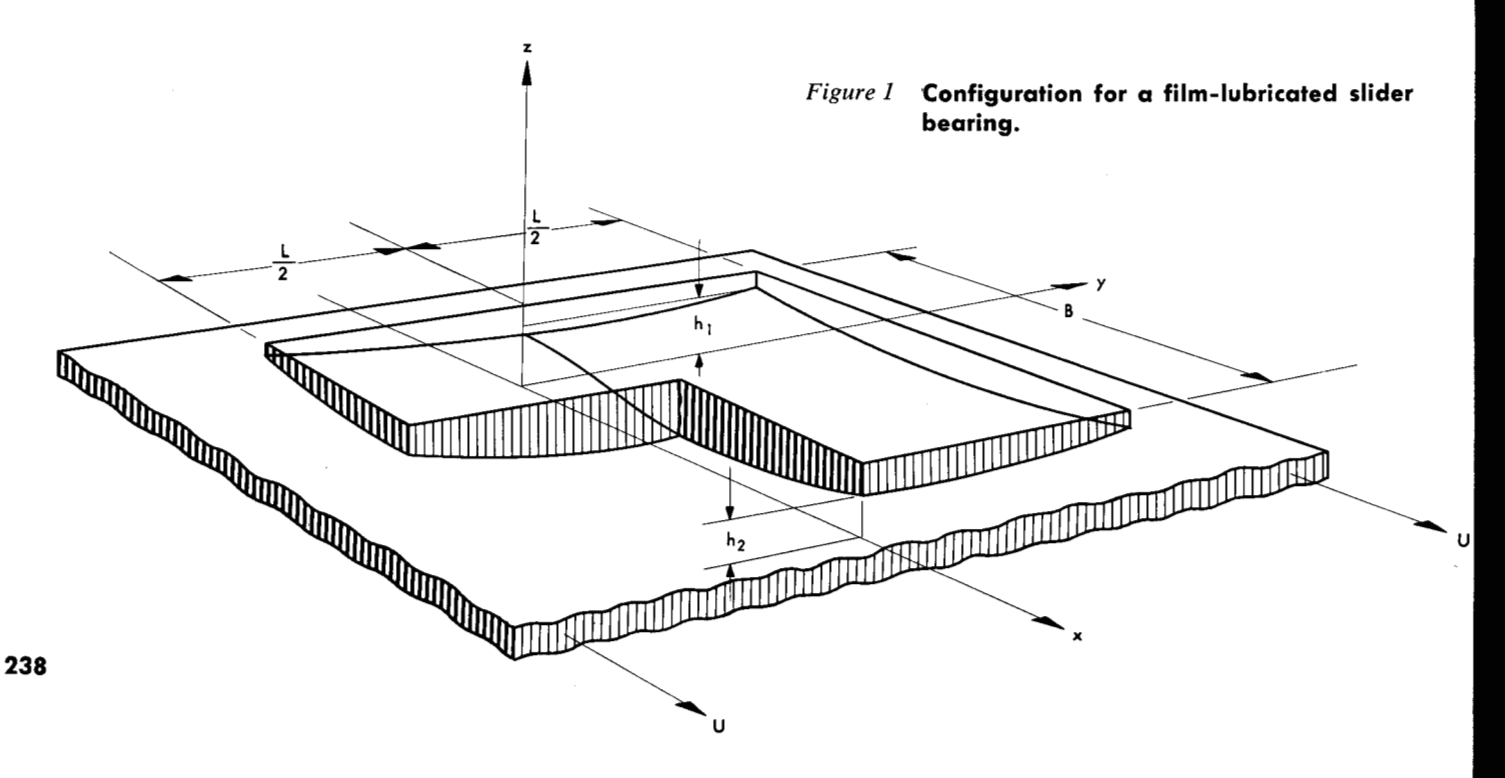
An order of magnitude evaluation of Eq. (6) reveals that the transverse pressure variation through the film may be ignored.

Upon removing constant translation components, the most general velocity boundary conditions become: $\mathbf{V}(z=0) = \mathbf{i}U_0 + \mathbf{j}V_0 + \mathbf{k}W_0$, $\mathbf{V}(z=h) = \mathbf{i}U_h + \mathbf{j}V_h + \mathbf{k}W_h$. When h > 25l (the molecular mean free path is l), boundary slip may be neglected and the fluid velocity at the boundaries assumed identical to the surface velocity. It is additionally assumed that surface asperities do not materially affect the films. Assuming steady conditions, and that the transverse density variation through the film may be neglected, Eqs. (3) and (6) may be combined to give

$$\left[\frac{\rho h^{3}}{\mu} p_{x}\right]_{x} + \left[\frac{\rho h^{3}}{\mu} p_{y}\right]_{y} = 6\left\{2h\rho_{t} + 2\rho(W_{h} - W_{0})\right. \\
\left. -\rho[(U_{h} - U_{0})h_{x} + (V_{n} - V_{0})h_{y}]\right. \\
\left. + h\{[\rho(U_{h} + U_{0})]_{x} + [\rho(V_{h} + V_{0})]_{y}\}\right\}, \tag{7}$$

the Reynolds equation for a laminar Newtonian fluid with $R^* << 1$.

The isothermal pressure distribution may be obtained from the Reynolds equation when h(x, y), the boundary conditions, and fluid properties are specified. Normally, edge effects are ignored, and the pressure is assumed to be ambient, p_a , for x=0, B, $y=\pm L/2$. Pressure distributions beyond this region have no physical meaning. It is tacitly assumed that a fully developed boundary layer exists throughout the film.



There is, of course, a wide variety of applications for Eq. (7). The range extends from high-capacity oil-lubricated thrust bearings to lightly loaded high-speed gas-lubricated bearings. Additionally, it is possible to apply Eq. (7) to journal bearings because the radial clearance is small compared to the radius. Under these conditions, the x coordinate is replaced by $r\theta$.

When bearing loads are large, the variation of viscosity with pressure and temperature, and therefore with spatial position, must be considered. Furthermore, although liquids are commonly assumed to be incompressible, the density of ordinary lubrication oil must at times be considered a function of pressure, as well as temperature. Under these conditions, the energy equation (4) must be adapted to the particular conditions, and solved simultaneously with the Reynolds equation (7) with due regard for parameter variations.

When Eq. (7) is to be applied to gas lubrication, it is also important that the energy equation (4) be considered. Under many lightly loaded conditions, it is justified to assume the lubricant to be isothermal. The consequence is that Eq. (7) may be modified by using Eq. (5) with T=Ta. Assume further (and in the sequel unless mentioned to the contrary) that conditions are steady in time, and the only non-zero velocity boundary condition is u(0) = U = constant. Then,

$$\left[\frac{h^3}{\mu} (p^2)_x\right]_x + \left[\frac{h^3}{\mu} (p^2)_y\right]_y = 12U[ph]_x, \qquad (8)$$

in which the term pp_x has been replaced by $(1/2)(p^2)_x$, and pp_y by $(1/2)(p^2)_y$.

When the lubricating fluid may be considered incompressible, the density terms of Eq. (7) vanish. The differential equation of the isothermal compressible film has the same form as the isothermal incompressible film. To use this similarity, it is necessary to relate p^2 and 2ph on the left and right sides of the compressible equation to the corresponding p and h of the incompressible equation,

$$\left[\frac{h^3}{\mu} p_x\right]_x + \left[\frac{h^3}{\mu} p_y\right]_y = 6[Uh]_x. \tag{9}$$

An approximation to Eq. (8) was integrated by W. J. Harrison.² In order to obtain his solution, Harrison assumed derivatives with respect to y to vanish, in effect describing an infinitely long bearing. This solution is for the case in which h is a linear function of x.

Because of the difficulties in handling the energy equation, it is common to use the pressure-density relation

$$p\rho^{-n}$$
 = constant, $1 \le n \le k$. (10)

The polytropic gas exponent is n. For isothermal conditions, n has the value 1, and for adiabatic, the value $k=c_p/c_v$.

A specific gas lubrication problem should be considered in the light of the energy equation (4). It is possible that sufficient information may be available about the flow conditions to reduce the energy equation to a tractable form. Equation (10), however, provides a simplifica-

tion which has allowed good correlation between theory and experiment. A more precise application of Eq. (10) would be to consider n=n(x, y).

By employing Eq. (10), the Reynolds equation may be written in the following forms,

$$\left[\frac{h^{3}p^{1/n}}{\mu}p_{x}\right]_{x} + \left[\frac{h^{3}p^{1/n}}{\mu}p_{y}\right]_{y} = 6U[p^{1/n}h]_{x}, \quad (11)$$

$$\left[\frac{h^{3}}{\mu}(p^{1+(1/n)})_{x}\right]_{x} + \left[\frac{h^{3}}{\mu}(p^{1+(1/n)})_{y}\right]_{y}$$

$$= \frac{6U}{n}(1+n)[p^{1/n}h]_{x}, \quad (12)$$

$$\left[\frac{h^{3}}{\mu} p_{x}\right]_{x} + \left[\frac{h^{3}}{\mu} p_{y}\right]_{y} + \frac{h^{3}}{\mu n p} \left[p_{x}^{2} + p_{y}^{2}\right]$$

$$= 6U\left[h_{x} + \frac{h}{n p} p_{x}\right]. \tag{13}$$

Once the pressure distribution has been obtained, it is possible to evaluate the shearing stresses on each surface,

$$\tau = \frac{\mu U}{h} \pm \frac{h}{2} p_x \,, \tag{14}$$

in which the (-) applies to the slider, and the (+) to the moving surface. The bearing load W, and the shearing force F, may be evaluated by integration. The shearing force on the moving surface should be used since it has the same magnitude as the shearing force on the slider plus the appropriate slider load component.

A coefficient of resistance sometimes used is defined:

$$f = F/W, \tag{15}$$

This has the order of magnitude of h/B.

Normalization of lubrication film equations

It is often desirable to work with normalized quantities. The dimensionless quantities shown in Table 1 will be used. The subscript *a* implies ambient conditions (inlet conditions for slider bearings).

Table 1 Dimensionless parameters.

Geometry	
Bearing breadth	1=B/B
Film thickness	$H\!=\!h/h_m$
x coordinate	X=x/B
y coordinate	Y=y/B
z coordinate	$Z=z/h_m$
Property	
Mass flow	$m'=m/p_ah_mLU$
Velocity	u'=u/U
Viscosity	$\Lambda = \mu/\mu_a$
Density	$\Gamma = \rho/\rho_{\alpha}$
Pressure	$P = p/p_a$
Bearing load	$W' = W/p_aBL$

Equation (13) may now be written in normalized form,

$$\left[\frac{H^3}{\Lambda} P_X\right]_X + \left[\frac{H^3}{\Lambda} P_Y\right]_Y + \frac{H^3}{\Lambda n P} \left[P_{X^2} + P_{Y^2}\right]$$

$$= G \left[H_X + \frac{H P_X}{n P}\right], \qquad (16)$$

in which the bearing number is $G = 6\mu_a UB/p_a h_m^2$.

It may be noted in passing that conventional dimensional analysis, taking into account the ambient pressure, minimum film thickness for a particular geometry, length, breadth, surface velocity, ratio of specific heats for constant temperature, and angle of inclination α , indicates that the bearing load W is a function of the following groupings:

$$W = pBLg_1\left(\frac{\mu U}{Bp}\right)g_2\left(\frac{B}{h}\right)g_3\left(\frac{L}{B}\right)$$
$$g_4\left(\frac{\mu U}{\rho c_p BT}\right)g_5(k)g_6(\alpha).$$

The bearing number G of Eq. (16) implies that the functions g_1 , g_2 , and g_3 may be combined to give $G^* = (6\mu_a U/Lp_a)(B/h_m)^2$. Both G and G^* have been effectively used for plotting load variations for fixed inclination slider bearings. For some configurations, it is convenient to replace h_m by $(h_1+h_2)/2$ or by $(h_1^2-h_2^2)^{1/2}$.

Examination of lubrication equations

It is instructive to examine the effect on load-carrying capacity and friction of liquid and gas-lubricating films as a result of the difference in viscosity and ambient pressure. The viscosity of a lubricating liquid may be a thousand times that of a gas. As a consequence, the load-carrying capacity and the frictional force will each be greater by approximately this factor for liquid lubrication than for gas film lubrication for equal bearing geometries.

If a lubricating film is incompressible, the absolute magnitude of the pressure is not related to the pressure changes. It is therefore possible to ignore atmospheric pressure when determining pressure variation. Thus, in Eq. (9), only derivatives of p occur. For compressible lubrication, this is not true because absolute pressure must be used (see Eqs. (4), (7), (11)). Increasing the ambient pressure of a compressible bearing film means that, although the ratio of maximum to ambient pressure decreases, the load-carrying capacity will increase.

Because of the nonlinear nature of the Reynolds equation for a compressible film, solutions may most easily be obtained by approximations such as linearizations. It is also possible to obtain qualitative information directly from the differential equation. For example, consider the pressure variation in the X direction. For simplicity, Eq. (7) may be applied to an infinitely long bearing so that the y-derivative terms vanish. If, in addition, the fluid is assumed to be incompressible, the density terms cancel, and the remaining equation may be immediately solved by elementary methods. If the lubricating fluid is compressible, it is possible to gain some comparative informa-

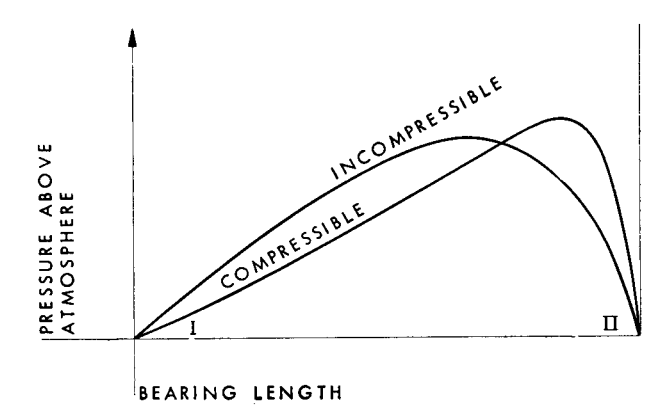


Figure 2 Comparative pressure distribution for compressible and incompressible lubrication.

tion by direct qualitative analysis of the differential terms.

A comparison of pressure variation for compressible and incompressible lubricating films may be recognized for the infinitely long bearing after integrating Eq. (7) once with respect to X. The result is

$$P_{X} = \frac{G}{H^{3}} \left(u'H - \frac{2m'}{\Gamma} \right), \tag{17}$$

in which m' represents the normalized mass rate of flow per unit length of the lubricant through the film, u' is the normalized velocity, and Γ is the normalized density. For the incompressible case, the ratio m'/Γ is the quantity of flow, a constant. To simplify comparison, consider the viscosity of the incompressible and compressible fluids to be the same. The pressure variation for the incompressible case is controlled now completely by the film thickness, H. Figure 2 illustrates qualitative pressure distributions for compressible and incompressible films. In Region I of the figure, P_X is positive, and in Region II, negative. It is zero for the condition $PH = m'/\Gamma$. For compressible lubrication, the increase in pressure is accompanied by a density increase. As a consequence, the term, m'/Γ decreases as P increases. Therefore, P_X increases more rapidly in the compressible film than in the incompressible. However, $P_X(0)_{\text{comp}} < P_X(0)_{\text{incomp}}$ so that $P_{\text{incomp}} > P_{\text{comp}}$ over the leading region of the film. In addition, for Region II, P_X and Γ_X are each negative, and the pressure of the compressible bearing must fall off more rapidly than that of the incompressible bearing. It follows therefore that the center of pressure will be farther from the leading edge of the bearing for the compressible than for the incompressible film.

Limiting characteristics of gas-lubricating films

It is possible to gain additional information from the Reynolds equation. When the bearing number is small $G\rightarrow 0$ (or, for a particular film geometry and constant viscosity, $U/p_a\rightarrow 0$), the pressure developed due to lubricating action can be only slightly different from p_a . Thus $P=p/p_a\rightarrow 1$, and the pressure derivatives are negligibly

small compared to the pressure magnitude. With these simplifications, Eq. (13) reduces to Eq. (9) the equation for an incompressible lubricating film.

Hence, for a given viscosity and film configuration, when the velocity is comparatively low, or the ambient pressure comparatively high, compressible and incompressible films behave similarly. For example, the load capacity varies linearly with velocity.

Now consider the other extreme, when the bearing number is large. For example, when $(U/p_a) \rightarrow \infty$, Eq. (12) may be written,

$$\left[\frac{H^{3}}{\Lambda}\left(P^{(n+1)/n}\right)_{X}\right]_{X} + \left[\frac{H^{3}}{\Lambda}\left(P^{(n+1)/n}\right)_{Y}\right]_{Y}$$

$$=G\left[\frac{n+1}{n}\right]\left[P^{1/n}H\right]_{X}.$$
(18)

It is first noticed that, as the right-hand side of Eq. (18) becomes large, the Y derivative terms become small compared to the X derivative terms. It follows that, for large bearing numbers, the lubrication of a finite bearing may be described by the solution for an infinitely long bearing. In addition, for finite pressure to be developed under the condition $(U/p_a) \rightarrow \infty$, it is necessary that

$$(P^{1/n}H)_X \rightarrow 0$$
.

The pressure distribution therefore becomes

$$P_{(G\to\infty)} = (H_a/H)^n \,. \tag{19}$$

This may also be shown by examination of the mass flow for large bearing numbers.

As an example of limiting load characteristics, a plane rectangular slider bearing will support a load

$$W' = W/p_a B L = \frac{H_1(H_1^{n-1} - 1)}{(n-1)(H-1)} - 1.$$
 (20)

Note that the equations for pressure and load involve neither speed nor viscosity. The load is carried by the compressibility effect of the ambient gas.

Since boundary layer characteristics are well known, a comparison between compressibility effects in a lubricating film and in a boundary layer is in order. For a Mach number as low as 0.25, compressibility, to the exclusion of the viscosity effects, may be of primary importance in the former, but of negligible importance to the latter.

In order to obtain a first approximation to a solution for a particular gas bearing configuration, asymptotic bounds may first be established for limiting values of U/p_a . The upper limit, established by Eq. (20) for the plane bearing will be considerably higher for adiabatic than for isothermal films. Thus it is important to establish an appropriate value for n. Experiments with slider bearings having about one square inch area reveal that a temperature rise at a thermocouple potted into the bearing surface is less than $4^{\circ}F$. Although the temperature within the film may be expected to rise higher, still the total effect upon density and viscosity appears to be negligibly small. The assumption of isothermal flow for slider

bearings appears to be justified. However, experiments upon gas lubricated journal bearings by Wildmann³ when compared with the theoretical solutions of Ausman,⁴ reveal that, from a load standpoint, journal bearing gas films appear to be nearly adiabatic.

For low bearing numbers, the results of incompressible lubrication studies may be used. Solutions for the finite, rectangular, plane slider bearing with an incompressible lubricating film have been given by Michell,5 Muskat, Morgan and Meres,6 Frössel7 and Wood.8 Solutions for rectangular slider bearings with curved surfaces have been provided by Boegli,9 Frössel,7 and Ying, Charnes, and Saibel.¹⁰ Raimondi and Boyd,¹¹ and Abramovitz¹² have studied the infinitely long curved slider bearing. The infinitely long slider bearing with a step was analyzed by Rayleigh,13 and the rectangular finite step bearing by Archibald.14 Solutions for the infinite tapered land bearings have been discussed by Bower.15 A wide variety of forms have been analyzed by Tipei. 16 The presently available solutions for compressible slider bearings are those due to Harrison,2 Constantinescu,17,18 Scheinberg,19 Tipei,16 and Kochi.20

For incompressible lubrication, it has been pointed out that the bearing friction is related to the bearing load by the same ratio as the minimum film thickness to the bearing length. This, of course, holds for compressible lubrication when U/p_a is small. However, as U/p_a increases and the asymptotic value of bearing load is approached, the frictional force continues to increase linearly with velocity. The consequence is that the coefficient of resistance, F/W, becomes increasingly less favorable for the compressible film, compared to the incompressible.

Some dynamic bearing effects

Slider bearings are usually used to provide thrust or for accurately maintaining specified film thicknesses. For thrust requirements, the important criteria are commonly the bearing load and frictional characteristics. For maintaining a constant-thickness film, it is necessary to specify other conditions. Specifications for high load-carrying capacity, minimum friction, and constant film thickness are generally combined in varying proportions for specific applications.

A bearing which will maintain a sufficiently uniform film thickness in the presence of anticipated accelerations in the z-direction, is said to have adequate stiffness. The term stiffness may be misleading because the damping characteristics of a lubricating film should not be ignored through concentration on the spring-like behavior of the film.

The load carried by a slider bearing resulting from the dynamic or squeeze film effect varies approximately inversely with the cube of the film thickness, whereas the hydrodynamic load capacity varies approximately inversely with the square of the film thickness. A qualitative load clearance curve, with the design clearance h_d and the design load W_d , is seen in Fig. 3. During anticipated operation, $W \approx W_d$ and $h \approx h_d$ so that the load-clearance curve

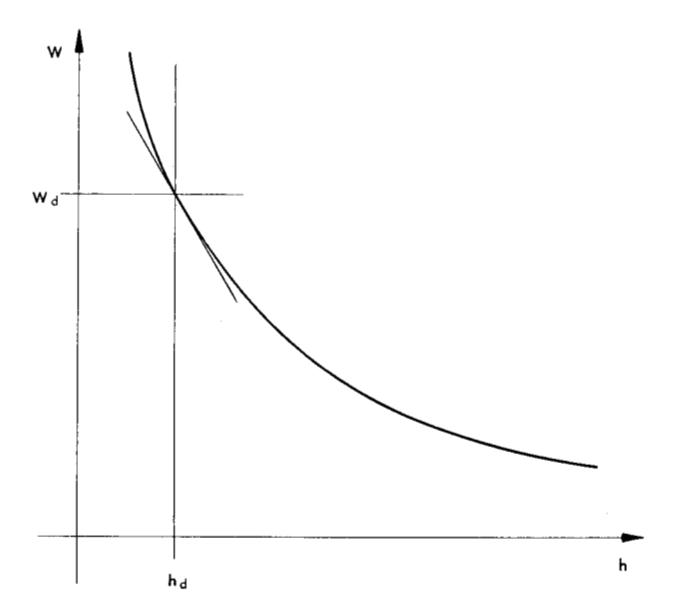


Figure 3 Load-clearance characteristic of slider bearing.

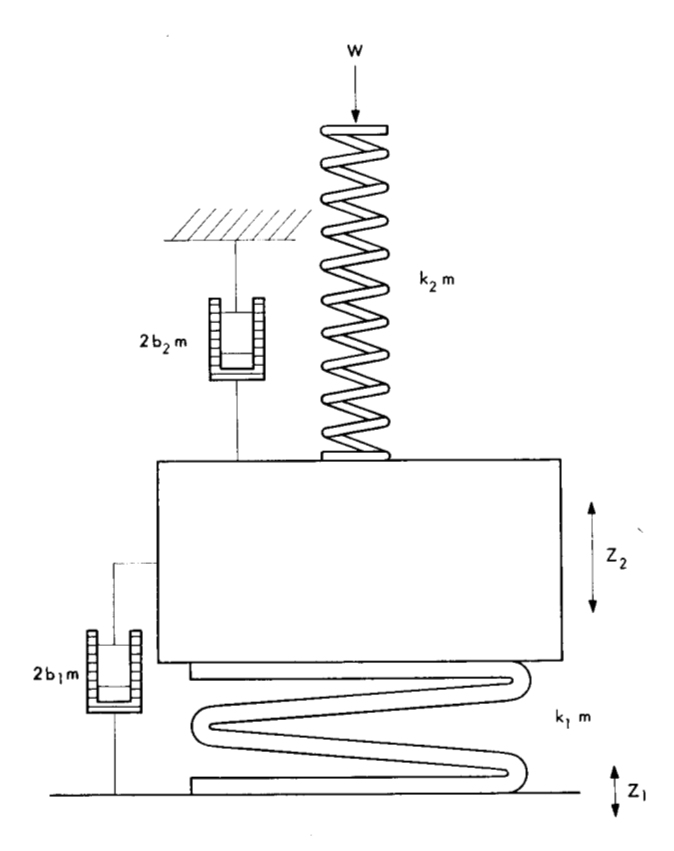


Figure 4 Equivalent dynamic system for springloaded slider bearing.

may be approximated by a straight line as illustrated. The inertia of a lubricating film is sufficiently small that the load-clearance results obtained for zero acceleration may ordinarily be used in the presence of acceleration. The squeeze film damping may similarly be linearized.

The result of these linearizations is to allow representation of the bearing as a single degree of freedom linear vibrating system as shown in Fig. 4. The spring represents the slope of the load displacement curve of the bearing for the particular operating conditions, and the dash pot represents the effect of the squeeze film. The mass, m, is the effective mass of the slider bearing. The equation of motion for the system is

$$Z_{2tt} + 2(b_1 + b_2)Z_{2t} + (k_1 + k_2)Z_2 = 2b_1Z_{1t} + k_1Z_1$$
, (21)

in which k_1 and k_2 are the equivalent spring constants of the lubricating film and loading mechanisms respectively, and $2b_1$ and $2b_2$ are the corresponding equivalent damping constants. More precisely, these constants are a function of the frequency at which the system is excited. Often, $k_1(Z_2-Z_1)>>k_2Z_2$, and $b_1(Z_2-Z_1)>>b_2Z_2$ so that the characteristics of the loading mechanism may be ignored.

The solution to Eq. (21) is well known. Usually the system is more than critically damped, so that there are no oscillatory characteristics. For maximum spacing control, frequencies of anticipated disturbances must be small compared to the undamped natural frequency, $k_1^{1/2}$. Thus the slope of the load spacing curve in the operating region becomes of primary importance.

Pivoted slider bearings

Pivot-loaded slider bearings have unusual characteristics. The angle of inclination of this type of bearing may automatically adjust so that, for any load, the center of pressure is always at the pivot. The difference in behavior between a pivot-loaded plane surface bearing with incompressible and compressible films is of particular importance.

With an incompressible film, the flat pivoted bearing will react to load changes as shown in Fig. 5. Under these conditions, the ratio of inlet to outlet film thickness remains constant. This may be verified by examination of the available theoretical solutions, or by experiment.

With a compressible film, the results can be strikingly different. Figure 5 illustrates the effect of load changes for particular operating conditions. A plane through the bearing passes through an area situated above the moving surface. It develops that there are two clearances possible for a particular load. One is stable, the other unstable. There is also a maximum load which may be supported. When the bearing is parallel to the moving surface, it is incapable of supporting a load and will therefore collapse. This effect was first experienced during experimental studies as discussed in Part III. The computer program, as described in Part II, was applied to this problem and yielded excellent verification of the experimental characteristics.

Collapse of the lubricating film will not occur for a

pivot-loaded convex curved surface because, neglecting the effect of asperities, a wedge may always be developed. Film collapse will not occur under pivoted Rayleigh-type step, or tapered land bearings. The superiority of these shapes over the plane surface bearing for many applications, such as support for magnetic elements, is apparent.

Solution of Reynolds equation

The theoretical solutions to slider bearing problems are generally complicated enough to warrant the use of digital computers, especially if many numerical results are required. This, of course, raises the question: Why not solve directly a difference equation which corresponds to the Reynolds differential equation? It appears at present that this is the most practical approach, even though hand relaxation must be used for all but the most simple geometrical configurations. As previously indicated, the rectangular slider bearing with plane and curved surface has been thoroughly investigated for incompressible lubrication. Unfortunately, the resulting equations are quite complex. When results are desired for unusual configurations, such as steps which curve in the bearing plane, or shapes other than rectangular (sectorial), the digital computer may be effectively used.

For compressible lubrication, the nonlinearity of the Reynolds equation places even more severe limitations on the theoretical solutions. This means that, for most gas lubrication problems, a direct approach by hand relaxation, or by using a digital computer, is the only available nonexperimental way to obtain accurate solutions. Part II discusses the finite difference technique by which a digital computer was used to approximate a solution to the Reynolds equation for gas-lubricated slider bearings. Accuracy of solution is discussed there.

Effects of parameter variations

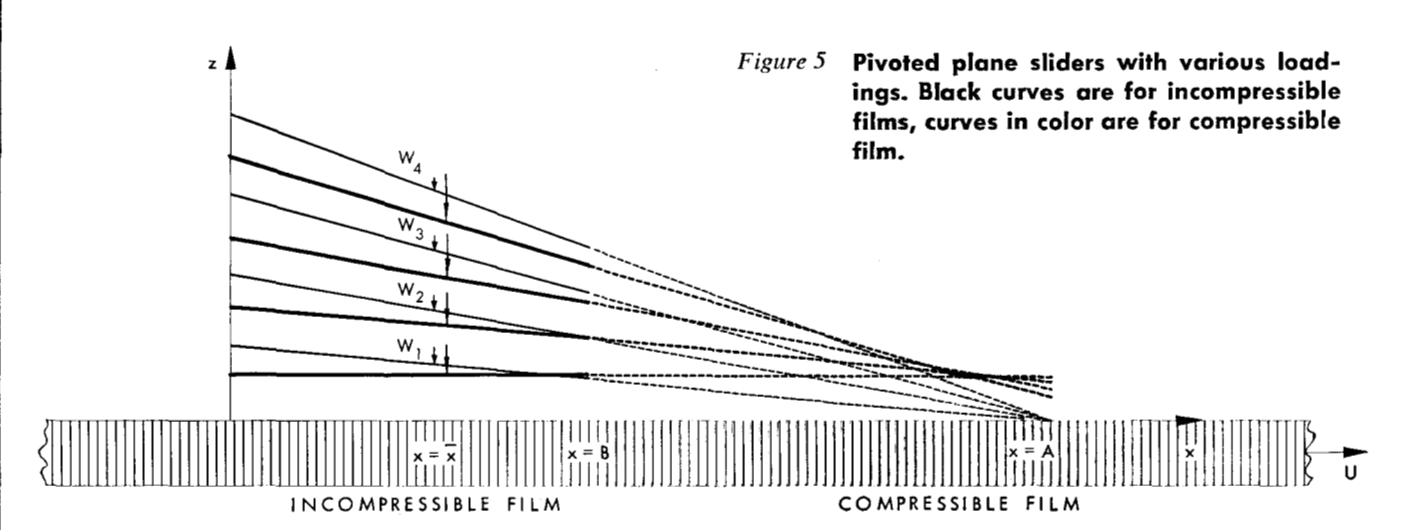
The interaction of the several bearing parameters makes the optimum design of a gas-lubricated slider bearing a difficult task. The bearing number, pivot position or angle of inclination, loading, shape and size as well as dynamic characteristics must all be considered. The effect of these parameters upon certain gas lubricating films will be illustrated in the ensuing figures. In every case, surfaces are considered to be perfectly smooth and the velocity of the moving surface is assumed to be steady in time. Curves are shown based upon results obtained using a digital computer programmed by Dr. W. A. Michael as described in Part II.

Three bearing shapes were considered: plane, cylindrically curved, and spherically curved. Pressure distributions and loads are presented for a variety of conditions. Pivot-loading and fixed-angle curves are shown from which equivalent stiffness may be determined. In addition, the effect of fixing either pivot position, minimum film thickness, or load of pivoted sliders is illustrated.

The film thickness for bearings with cylindrical or spherical surfaces is represented by $h=h_0+a^2/2R+(a/R)x+(2R)^{-1}x^2+(2R)^{-1}y^2$ in which the radius of curvature is R. There is of course no y variation for cylindrical surfaces. The inlet film thickness is $h_1=h(x=0)$, and the outlet film thickness is $h_2=h(x=B)$. The minimum spacing between the parabola which defines the curved surface and the driving surface, h_0 , occurs at x=a. In case the parabolic arc subtended by the curved surface does not include the minimum spacing, a>B and $h_2=h_m>h_0$. The crown height δ is the perpendicular distance of the vertex of the surface in the plane of symmetry of the bearing, to the line connecting the inlet and trailing edges.

It is possible to normalize cylindrical bearing films by relating film thickness to h_0 and lengths to $(2h_0R)^{1/2}$. Results may then be compared for any combination of R and h_0 as long as a $(2h_0R)^{-1/2}$ and $B(2h_0R)^{-1/2}$ remain fixed. This type of comparison is impractical for this study. Hence crown height is normalized with respect to minimum film thickness and length to B. Some selected numerical data are tabulated in an internal IBM report.²¹

The well-known Harrison solution for the infinitely long isothermal plane inclined slider bearing provides a useful first step toward analysis or synthesis of gas-bear-



ing films. The solution is sufficiently complicated that Figs. 6, 7, and 8 are presented to illustrate the effects of inclination $(H_1=h_1/h_2=1.5, 3, 6)$, and bearing number upon isothermal pressure distribution for infinitely long films. Numerical data for pressures at twelve position intervals are presented in the aforementioned internal report. ²¹ Curves for the corresponding center of pressures are shown in Fig. 9. An additional normalization is possible by dividing P by H_1 . However, such normalization appeared to be undesirable for this investigation.

Figures 10 and 11 illustrate the effect of bearing number and film thickness ratio upon isothermal load for various fixed plane inclined sliders. Bearing length ratios of ∞ and 2 are illustrated so that side flow factors may be determined for these examples. Figure 12 illustrates the effects of bearing number, inclination, and gas expansion characteristics upon load for fixed plane sliders having length ratios L/B=1. In addition to isothermal and adiabatic (for air and helium) load curves, characteristics for incompressible films are shown. The asymptotic loads for $G\rightarrow\infty$ are marked. All compressible curves for $G\rightarrow0$ are asymptotic to the appropriate incompressible load line. Adiabatic (air), as well as incompressible load curves, are shown.

Figure 13 may be used in connection with Figs. 10 and 12 to evaluate the effect of bearing length ratio upon load for fixed plane inclined sliders, for which $H_1=2$. Isothermal and adiabatic (air) curves are shown.

Figures 14 and 15 may be compared to evaluate the effects of curvature upon load for fixed sliders, for which $H_1=2$, and L/B=1. Results are presented for both cylindrical and spherical sliders with different curvatures. Isothermal and adiabatic (air) conditions are presented.

A careful scrutiny of the region $G \rightarrow 0$ of Figs. 14 and 15 reveals that, although asymptotic to the incompressible load line, the compressible films support greater loads for certain conditions: $h_2 > h_m$ and G sufficiently small. Under these conditions, the incompressible film develops pressures less than atmospheric (assuming the bearings to be submerged in the lubricant). Although the pressure peaks of the compressible film are not so high as those of the incompressible film, the pressure remains always above ambient so that the total load supported is greater than that of the incompressible film. Figures 16 and 17 illustrate pressure distributions for incompressible and isothermal films for cylindrical sliders for which G=18.57, $\delta/h_m = 0.5$, $H_1 = 2$, and $h_2/h_m = 1.17$. Figure 18 represents the pressure difference between the films of Figs. 16 and 17. The normalized load carried by the incompressible film, 0.2159, is 0.0244 greater than that of the incompressible film. The shift of the center of pressure is easy to visualize.

Figure 19 illustrates isothermal pressure distributions for cylindrical sliders for which G=22.50, L/B=1, and $H_1=3$. Similar curves showing isothermal pressure distribution for plane and spherical sliders have been determined and are available.²¹ The bearing number is chosen to be representative of operation approximately equally separated from the asymptotic regions $G\rightarrow 0$ and $G\rightarrow \infty$.

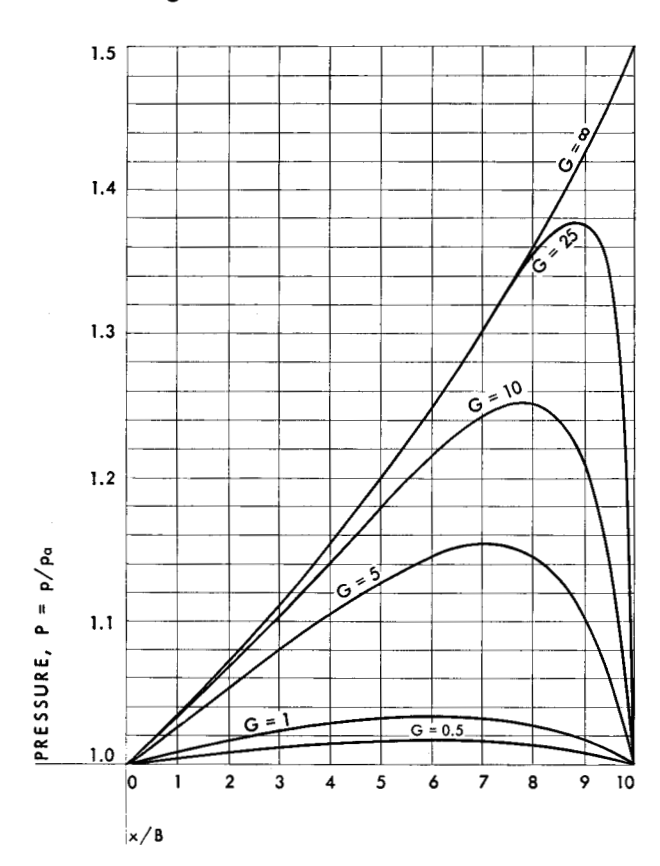
The pressure patterns have been plotted from data on 24×24 grids. Comparison solutions on 12×12 grids reveal changes less than one per cent.

Some of the characteristics of pivoted sliders may be recognized by observation of the remaining figures. Figures 20 and 21 illustrate the effects of isothermal load changes upon pivoted and fixed angle sliders. Results are plotted versus minimum film thickness, h_m . Equivalent stiffness may be obtained by measuring the slope of a $W'-h_m$ curve.

Figure 20 is particularly revealing. Load, angle of inclination, and film thickness ratio are plotted for a pivoted plane slider. The unstable region of operation, as previously discussed, is apparent. When the angle of inclination is zero, $(H_1=1)$, no load may be supported. However, the addition of an extremely small convexity is sufficient to guarantee a wedge for small film thicknesses so that the load capacity is ideally unlimited.

Figure 21 illustrates the similarity of load clearance characteristics of pivoted and fixed angle, slightly curved bearings. Both isothermal and adiabatic (air) conditions are shown for the latter.

Figure 6 Isothermal pressure distributions for infinitely long inclined slider bearings having film thickness ratio $h_1/h_2=1.5$.



The effect of increasing bearing number upon load, inclination, and minimum film thickness for a plane slider bearing having a fixed pivot position with respect to the driving surface is illustrated in Fig. 22. An optimum unit load condition is apparent.

The figures presented here may be used to establish approximate characteristics of gas-lubricated slider bearings. Computer and experiments may then be used to optimize the film. Additional work is in progress and will be reported in the future.*

List of Symbols

- b equivalent damping constant
- B bearing breadth in line with surface velocity
- c_p specific heat for constant pressure
- c_v specific heat for constant volume
- E intrinsic energy per unit mass
- F force on a differential element

 $G = 6\mu_a UB/p_a h_m^2$

- film thickness, clearance
- h_m minimum film thickness
- $H h/h_r$

h

- i unit vector in x direction
- j unit vector in y direction
- k unit vector in z direction
- k adiabatic gas expansion term $(k=c_p/c_v)$;
 - equivalent spring constant
- K thermal conductivity
- L bearing length normal to surface velocity
- m mass rate of flow per unit length through
 - lubricating film; bearing mass
- $m' = m/\rho_a U h_m$
- n polytropic gas expansion term
- $P = p/p_a$
- r radius of journal bearing
- R gas constant, radius of curvature
- R* modified Reynolds number
- t time

Subscripts a: ambient conditions; independent variables: partial differentiation with respect to the subscript.

Figure 7 Isothermal pressure distributions for infinitely long inclined plane slider bearings having film thickness ratio $h_1/h_2=3$.

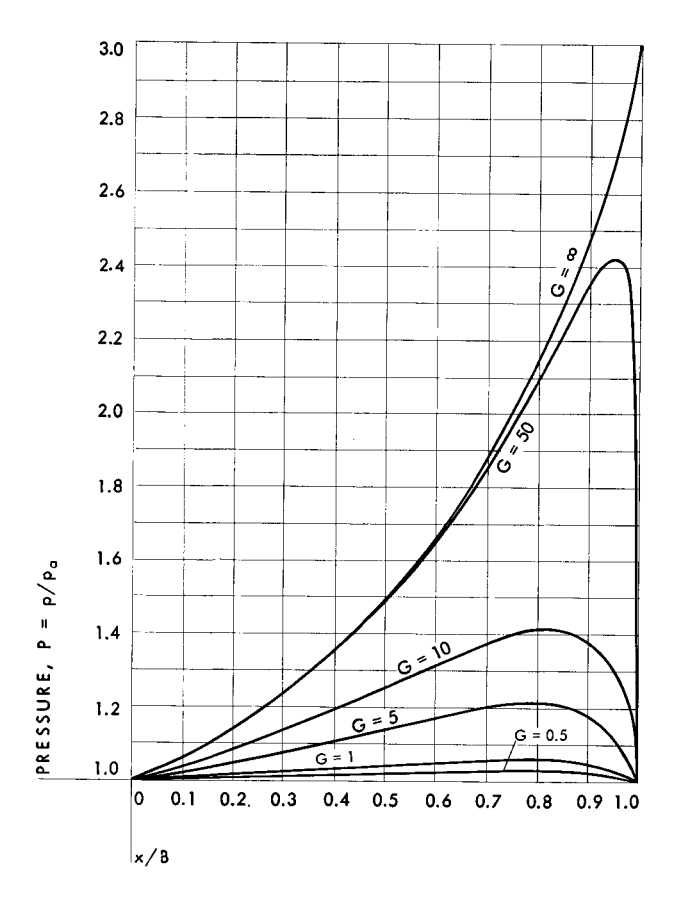
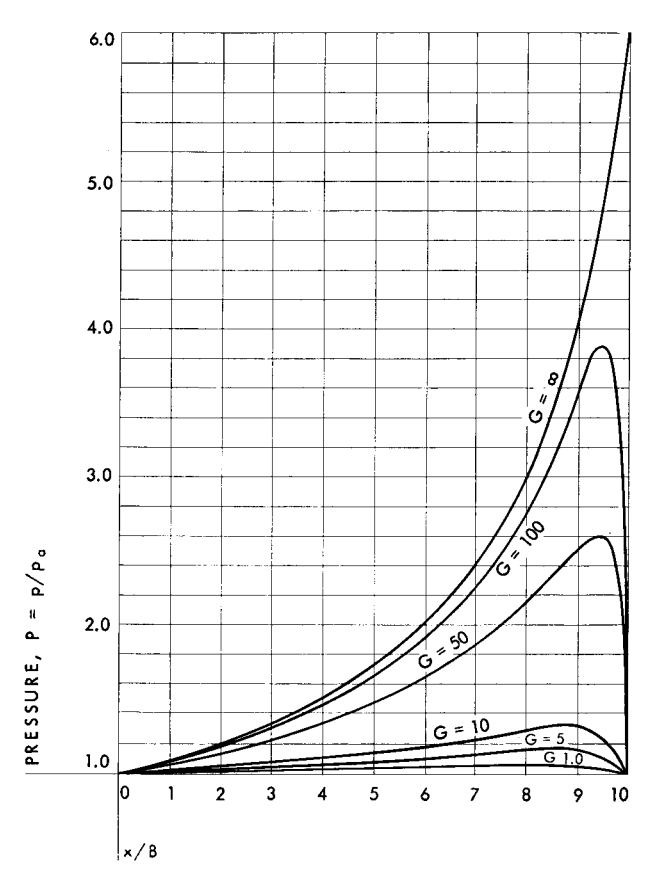


Figure 8 Isothermal pressure distributions for infinitely long inclined plane slider bearings having film thickness ratio $h_1/h_2=6$.



^{*}Paper to be presented at First ONR International Symposium on Air Lubrication, Washington, D. C., October 26, 27, 28, 1959.

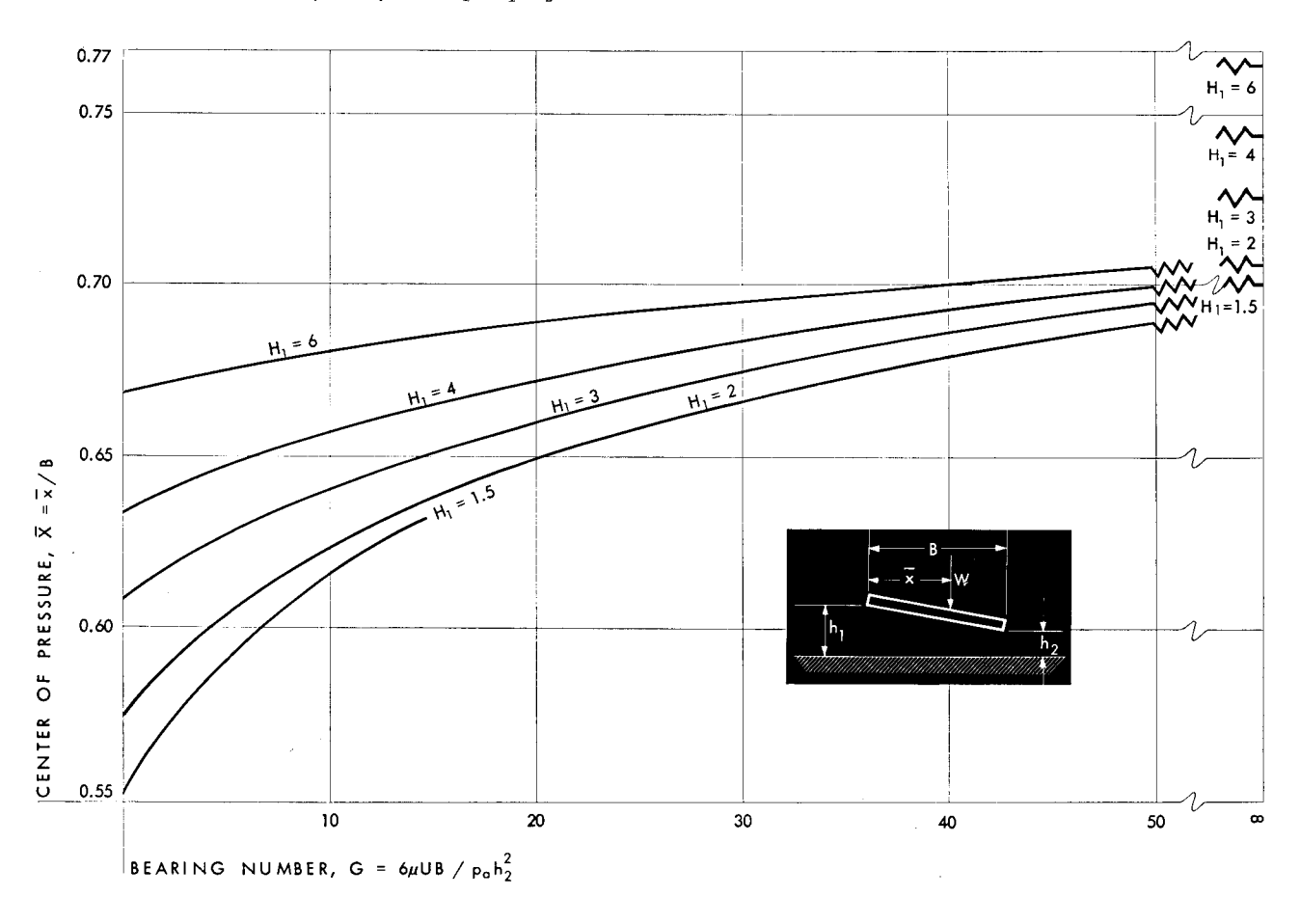
 \boldsymbol{T} temperature (absolute) $\boldsymbol{\mathit{U}}$ magnitude of driving-surface velocity in x direction magnitude of velocity component in x direction и u'magnitude of velocity component in y direction vvector velocity v magnitude of velocity component in z direction w W' $W/p_{a}BL$ x, y, z rectangular coordinates \boldsymbol{X} x/BY y/B \boldsymbol{Z} z/Bangle of inclination α Γ ρ/ρ_a θ angular variable Λ μ/μ_a λ coefficient of dilatational viscosity coefficient of viscosity μ density ρ shearing stress τ

dissipation function

References

- 1. O. Reynolds, "On the Theory of Lubrication," *Phil. Trans. Roy. Soc.*, 177, ser. A, 157 (1886).
- W. J. Harrison, "The Hydrodynamical Theory of Lubrication with Special Reference to Air as a Lubricant," Trans. Camb. Phil. Soc., 22, 39 (1913).
- 3. M. Wildmann, "Experiments on Gas-Lubricated Journal Bearings," ASME paper no. 56-LUB-8, ASME-ASLE Lub. Confr. (1956).
- J. S. Ausman, "Finite Gas-Lubricated Journal Bearing," Inst. Mech. Engrs., paper 22, London Confr. on Lub. & Wear (1957).
- A. G. M. Michell, "The Lubrication of Plane Surfaces," Z. Math. Physik, 52, 123 (1905).
- 6. M. Muskat, F. Morgan, and M. W. Meres, "The Lubrication of Plane Sliders of Finite Width," *J. Appl. Phys.*, 11, 208 (1940).
- 7. W. Frössel, "Berechnung der Reibung und Tragkraft eines endlich breiten Gleitschuhes auf ebener Gleitbahn (Calculation of Load and Friction of Smooth Surface Finite Slider Bearings)," Zeit. fur Ang. Math. u. Mech., 21, no. 6, 321 (1941).
- 8. W. L. Wood, "Note on a New Form of the Solution of Reynolds-Equation for Michell Rectangular and Sector-Shaped Pads," London, Edinb., and Dublin Phil. Mag. and Jour. of Sci., 7th series, 40, 220 (1949).

Figure 9 Effect of bearing number upon isothermal center of pressure for infinitely long plane slider bearing where $L/B = \infty$, n = 1, and $H_1 = h_1/h_2$.



246

Φ

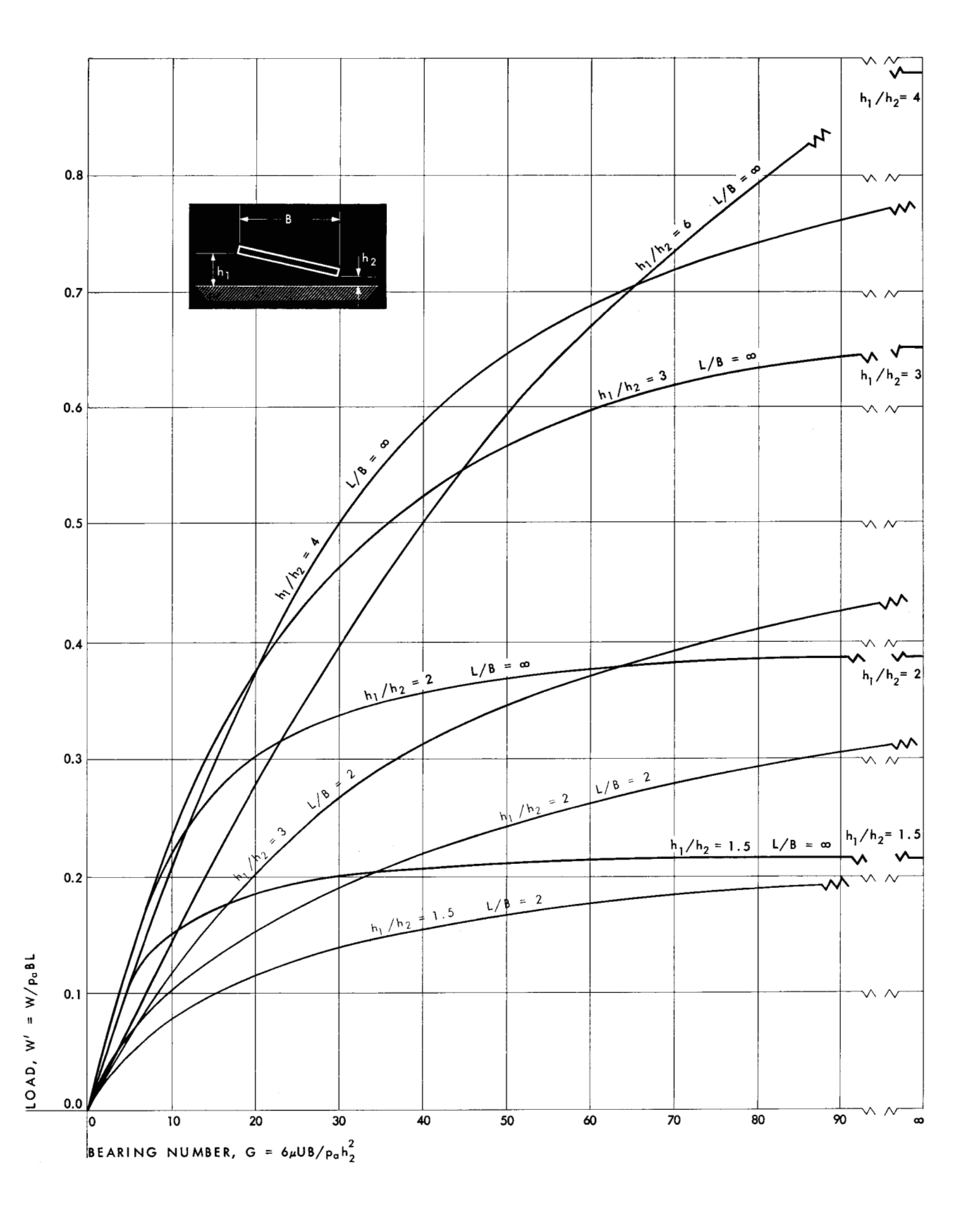


Figure 10 Effect of bearing number upon isothermal load for plane sliders having film thickness ratios $h_1/h_2=1.5$, 2, 3, 4, and 6 with $L/B=\infty$ and 2, and n=1. Curve for $h_1/h_2=6$ intersects infinity at W'=1.150. Both colored and black curves intersect infinity at points shown.

- 9. G. P. Boegli, "The Hydrodynamic Lubrication of Finite Sliders," J. Appl. Phys., 18, 482 (1947).
- A. S. C. Ying, A. Charnes, and E. Saibel, "Slider Bearing with Transverse Curvature; Exact Solution," Trans. Am. Soc. Mech. Engrs., 78, 465 (1956).
- 11. A. A. Raimondi, and J. Boyd, "The Influence of Surface
- Profile on the Load Capacity of Thrust Bearings with Centrally Pivoted Pads," *Trans. Am. Soc. Mech. Engrs.*, 77, 321 (1955).
- 12. S. Abramovitz, "Theory for a Slider bearing with a Convex Pad Surface; Side Flow Neglected," J. Franklin Inst., 259, 221, No. 3 (1955).

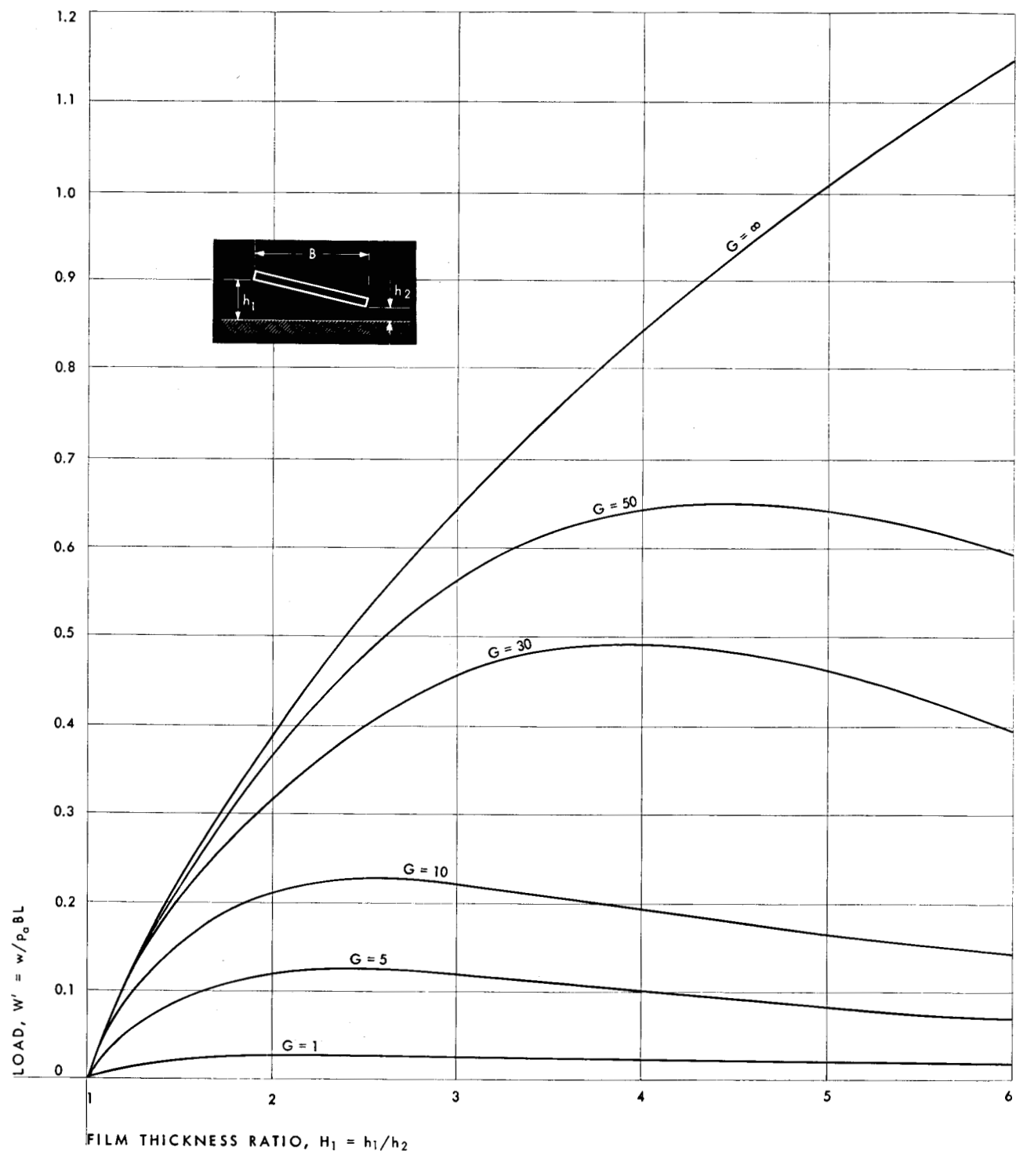


Figure 11 Effect of film thickness ratio upon isothermal load of infinite sliders for various bearing numbers with $L/B = \infty$, and n = 1.

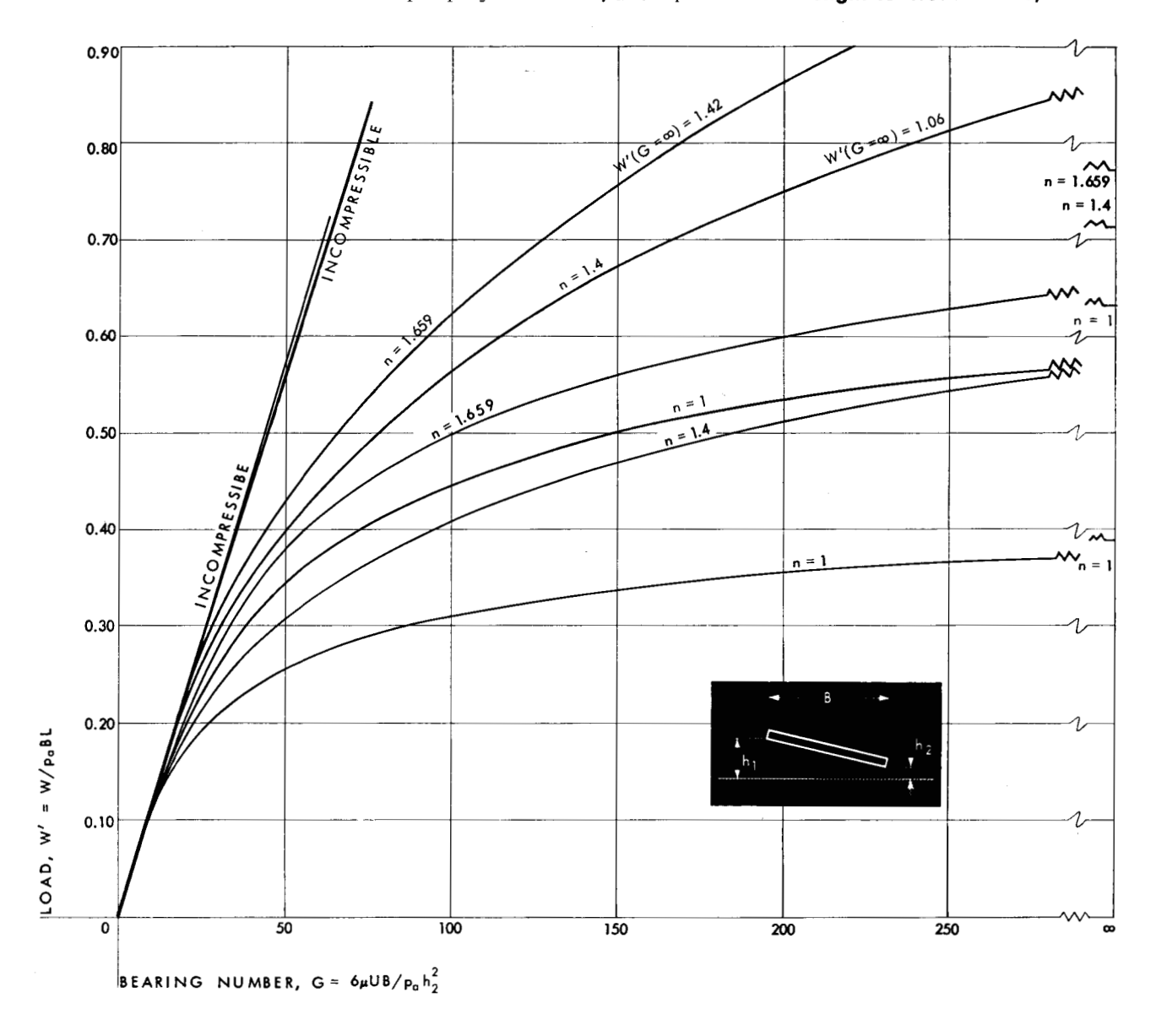
- 13. Lord Rayleigh, "Notes on the Theory of Lubrication," London, Edinb., and Dublin Phil. Mag. and Jour. of Sci., Sixth Series, 35, 1 (1918).
- F. R. Archibald, "A Simple Hydrodynamic Thrust Bearing," Trans. Am. Soc. Mech. Engrs., 72, 393 (1950).
- G. S. Bower (Discussion of Paper by A. Fogg), Proc. Inst. Mech. Engr., 155, 61 (1946).
- N. Tipei, "Hidro-Aerodinamica Lubrificatiei (Hydro-Aerodynamics of Lubrication" (in Romanian), Academiei Republicii Populare Romine (1957).
- V. N. Constantinescu, "Sur la Théorie des Paliers á Gaz (On the Theory of Gas Bearings)," Rev. de Mecan. Appliq., 1, no. 1, 141 (1956).
- V. N. Constantinescu, "Sur le Problème Tridimensionnel de la Lubrication aux Gas (On the Three Dimensional Problem of Gas Lubrication)," Rev. de Mecan. Appliq., 1, no. 2, 123 (1956).

- S. I. Scheinberg, "Gas Lubrication of Slider Bearings (Theory and Calculations)" (in Russian), Friction and Wear in Machines, Institute of Machine Sci. Acad. of Sci. USSR, 8, 107 (1953).
- K. C. Kochi, "Characteristics of a Self-Lubricated Stepped Thrust Pad of Infinite Width with Compressible Lubricant," Paper No. 58-A-194, presented at 1958 A.S.M.E. annual meeting.
- annual meeting.

 21. W. A. Gross, "A Gas Film Lubrication Study: Some Theoretical Analyses of Slider Bearings," IBM Research Paper RJ-RR-126 (1958).

Received June 19, 1958

Figure 12 Effect of bearing number upon isothermal and adiabatic (air, helium) load for plane slider bearing with film thickness ratio $H_1=h_1/h_2=2$ in black, and $H_1=3$ in color. Length-to-breadth ratio, L/B=1.





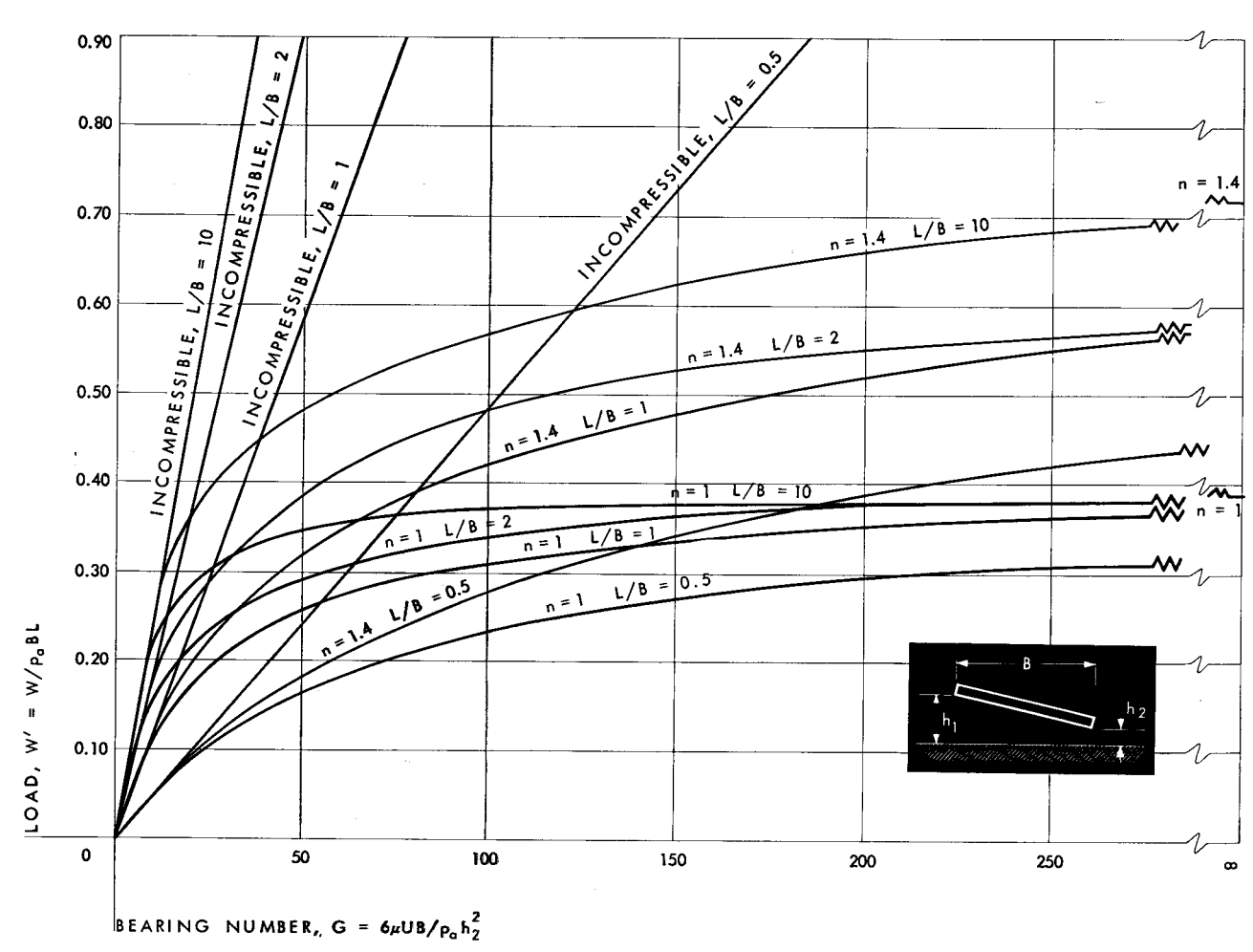


Fig. 14

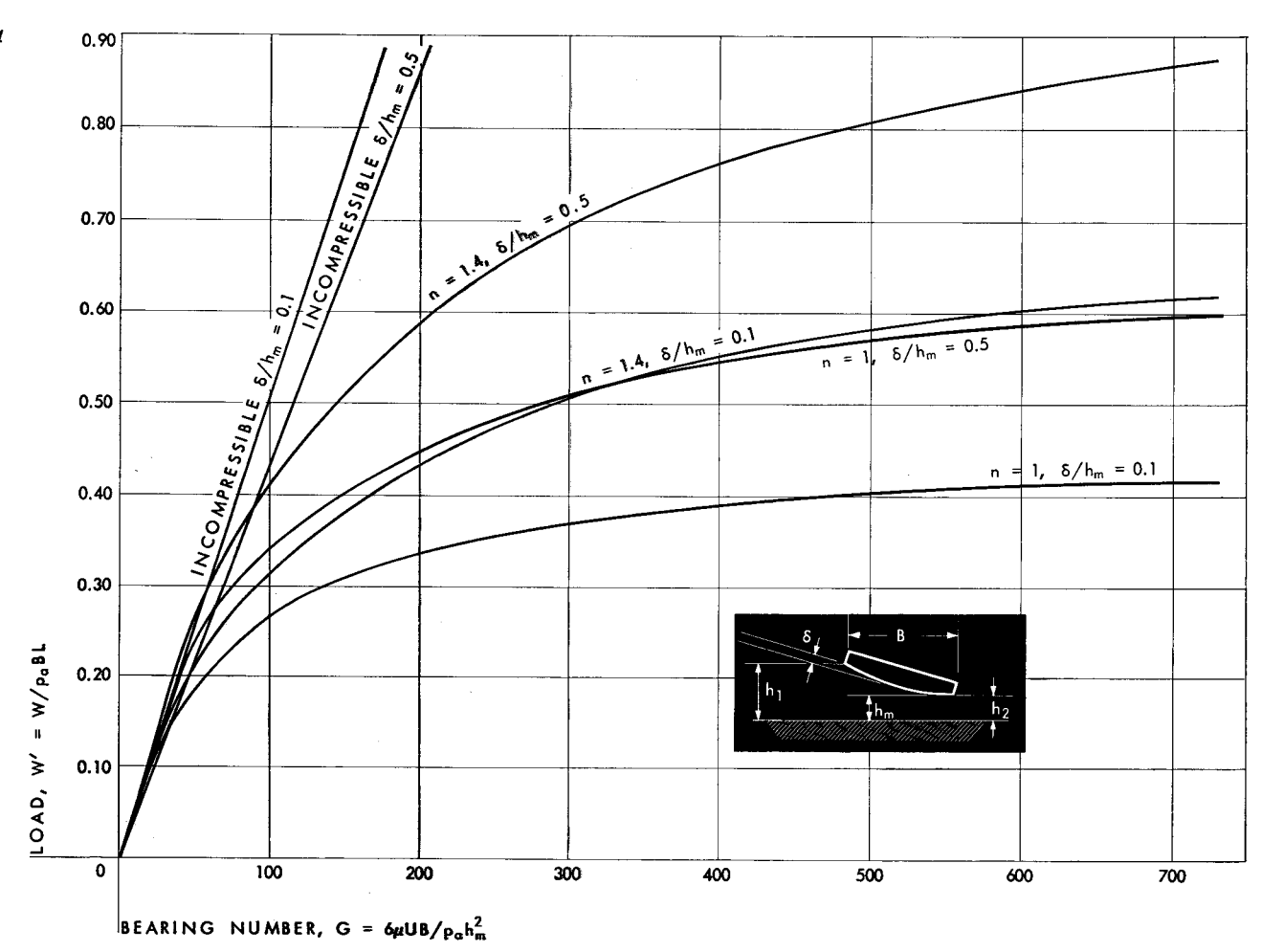


Figure 13 Effect of bearing number upon isothermal and adiabatic (air) load for plane slider bearings having film thickness ratio $h_1/h_2=2$, and different length-to-breadth ratios.

Curves in color are for n=1.

Figure 14 Effect of bearing number upon isothermal and adiabatic (air) load for convex cylindrical slider where L/B=1, $h_1/h_m=2$, and $\delta/h_m=0.1$ and 0.5.

Curves in color are for n=1.

Figure 15 Effect of bearing number upon isothermal and adiabatic (air) load for convex spherical slider where L/B=1, $h_1/h_m=2$, and $\delta/h_m=0.1$ and 0.5.

Curves in color are for n=1.

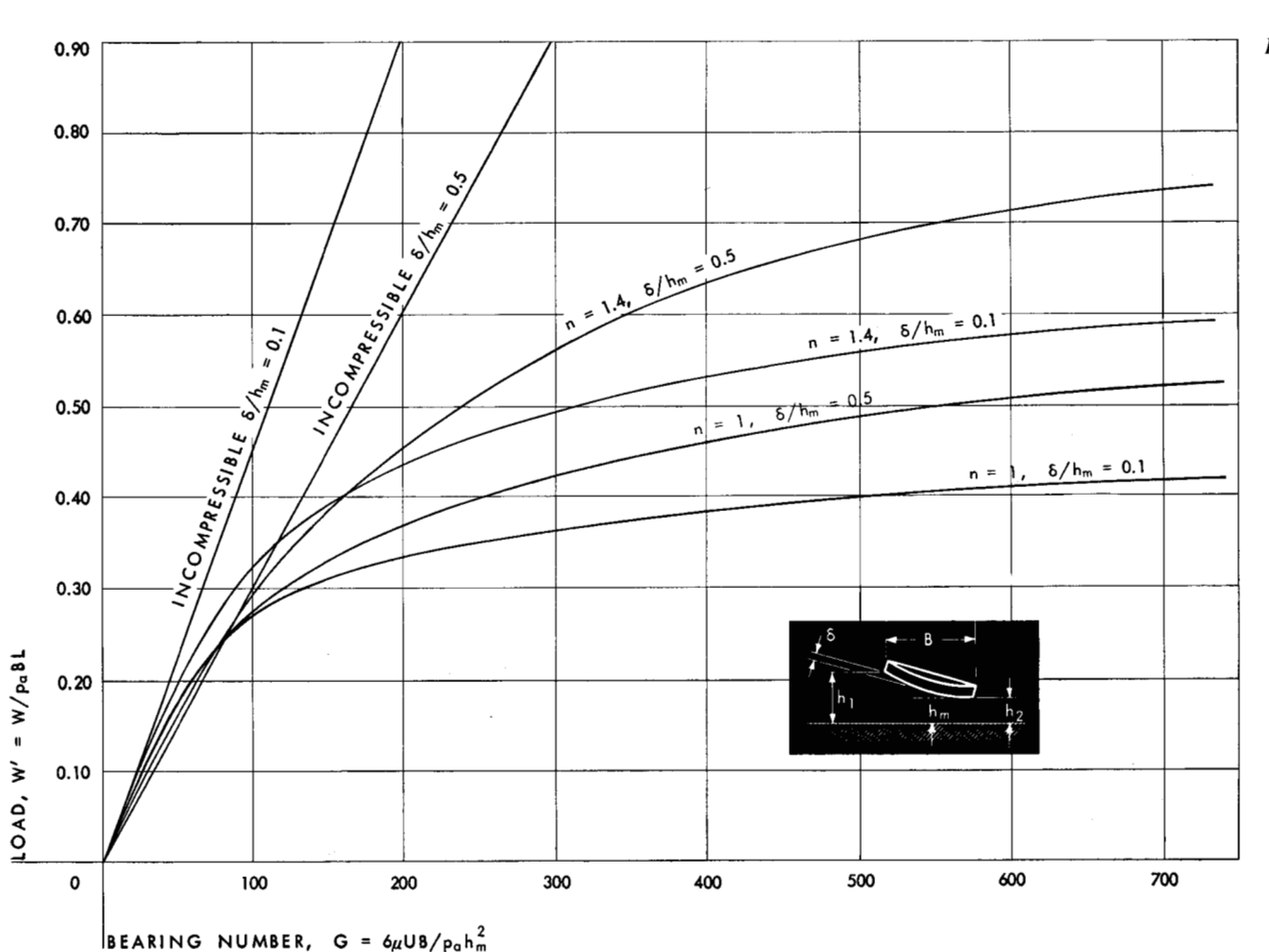
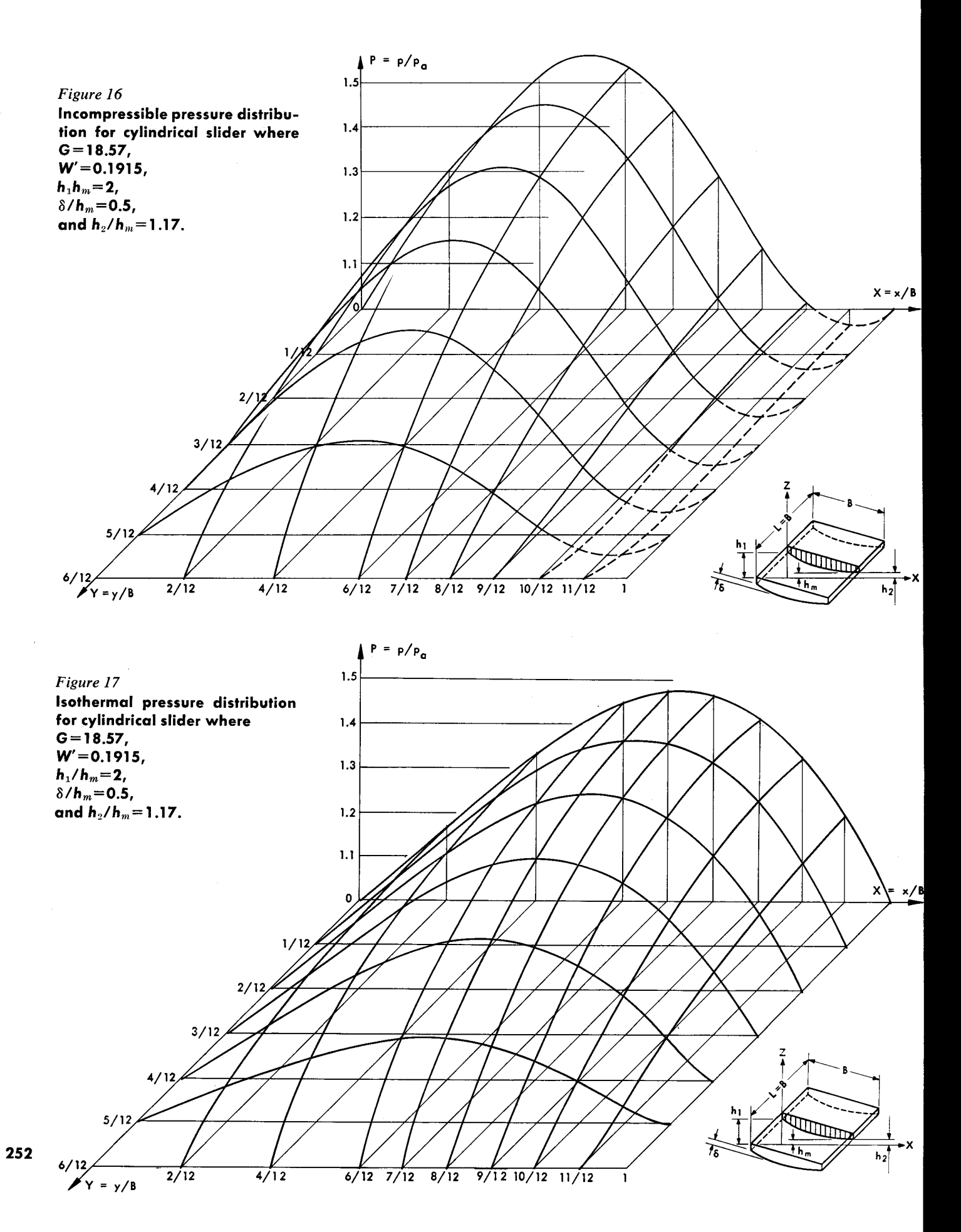
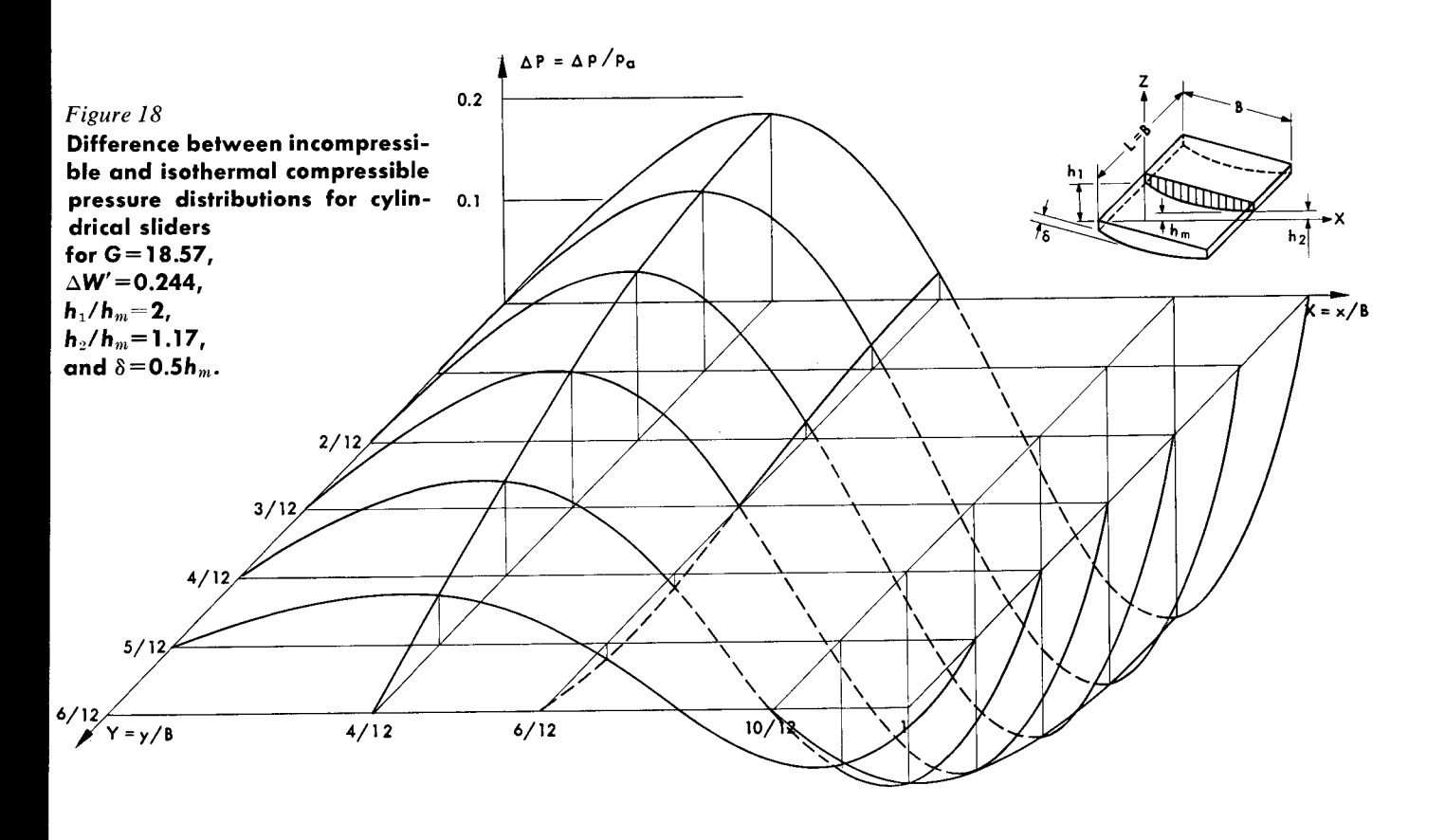


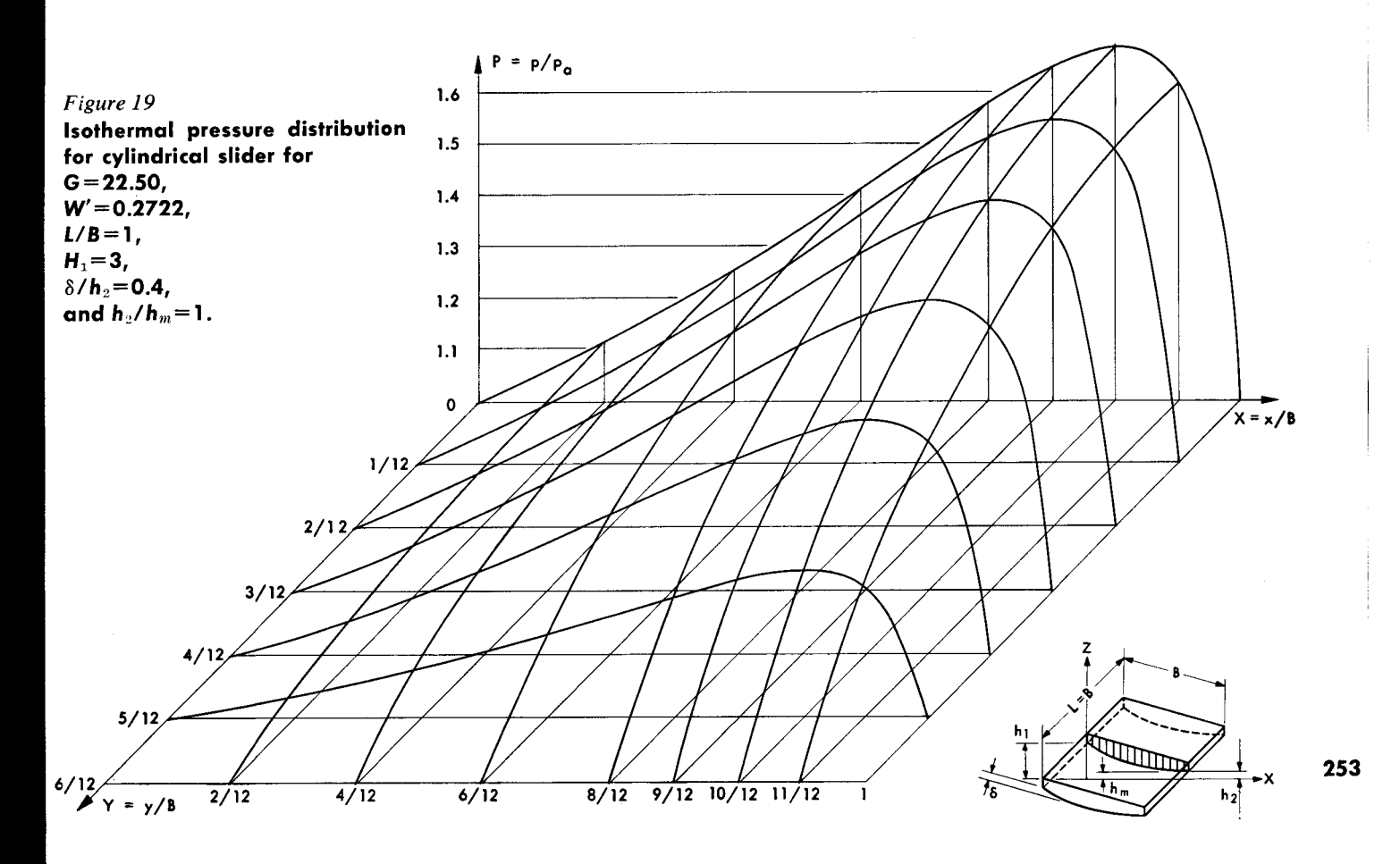
Fig. 15

251

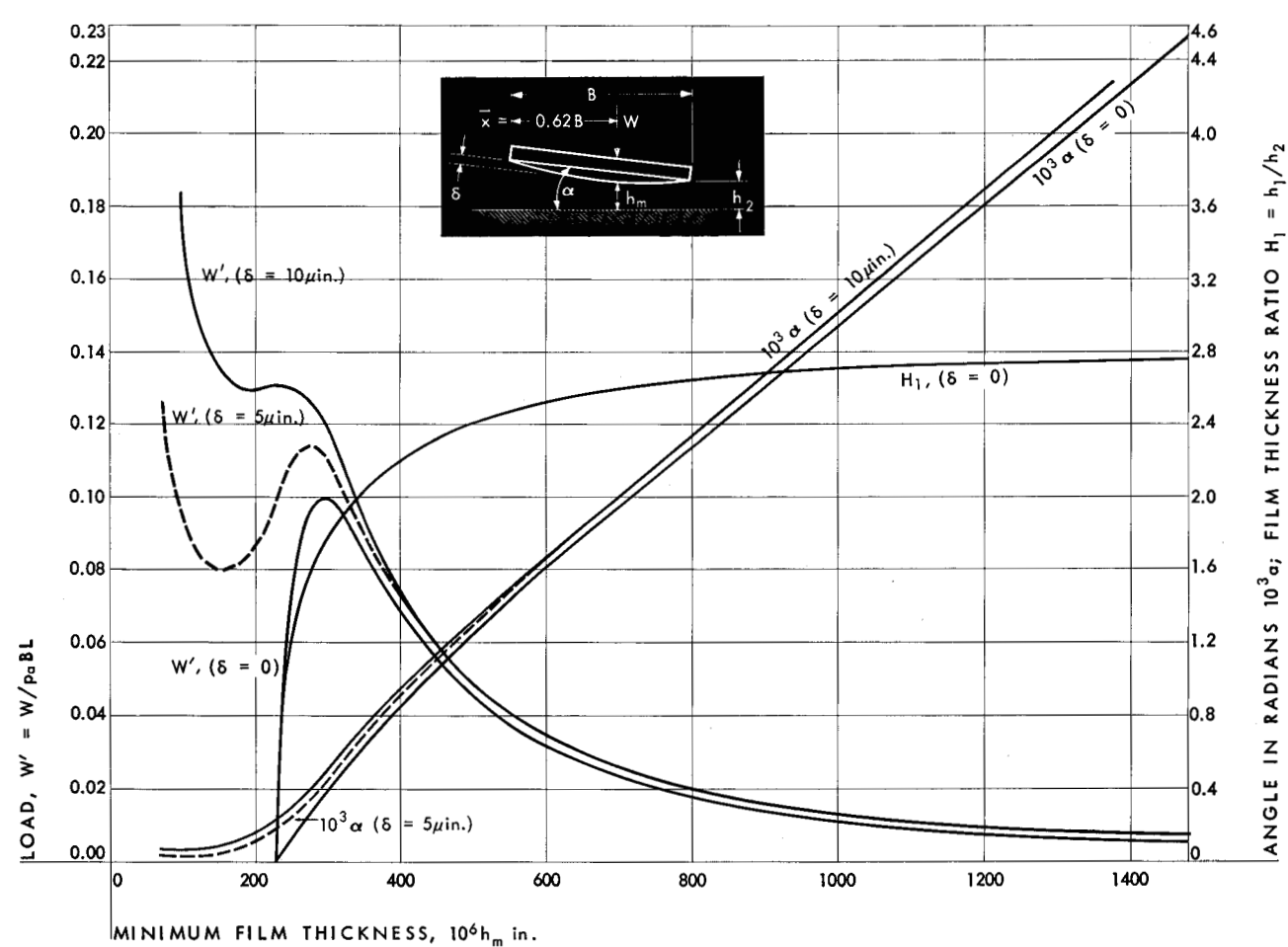
IBM JOURNAL • JULY 1959











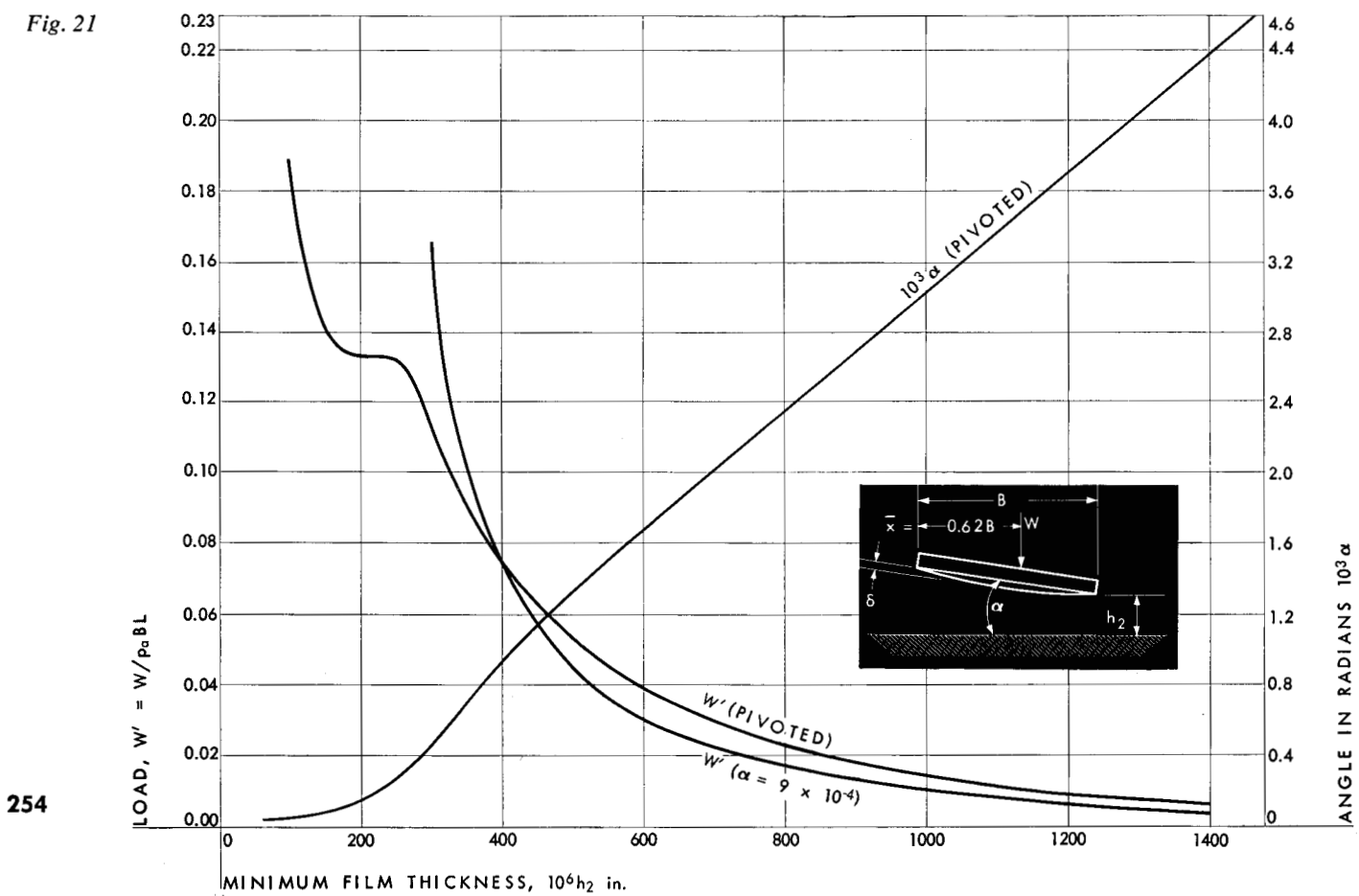
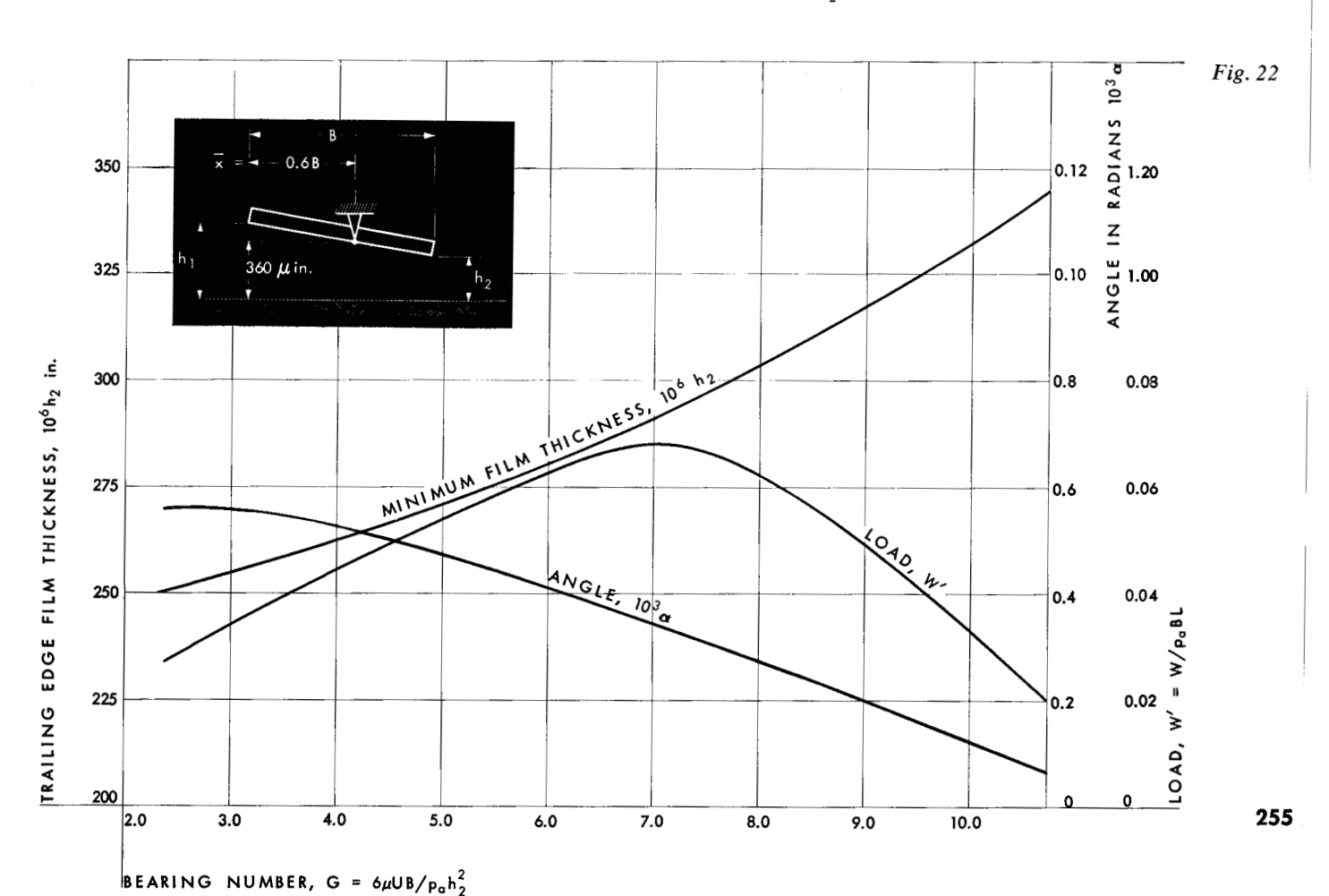


Figure 20 Effect of minimum film thickness upon isothermal load, angle, and film thickness ratio for plane and convex cylindrical pivoted sliders where L/B=1, $G=8.779\times 10^{-7}/h_n^2$, $h_1/h_2=1+0.578\alpha/h_2$, and B=0.578 in.

Figure 21 Effect of minimum film thickness upon load and angle for isothermal load and angle of a pivoted convex cylindrical slider, and for a similar fixed angle slider for $\delta=10\mu \text{in.}, L/B=1, G=8.779\times 10^{-7}/h_m^2, h_1/h_2=1+0.578\alpha/h_2$, and B=0.578 in.

Figure 22 Effect of bearing number upon angle of inclination, minimum film thickness, and bearing load for an isothermal film of plane slider with fixed pivot for L/B=1, μ/P_a 1.875×10^{-10} sec., and $h_1/h_2=1+0.5\alpha/h_2$.



IBM JOURNAL • JULY 1959